AGU PUBLICATIONS

Geophysical Research Letters

RESEARCH LETTER
10.1002/2014GL062210

Key Points:
- A new method quantifying baroclinic/barotropic eddy feedback in SAM introduced
- Barotropic processes drive and sustain SAM; baroclinic ones extend SAM persistence
- Wave activity drives SAM variability but feedbacks negatively for SAM persistence

Correspondence to:
Y. Zhang,
yangzh@alum.mit.edu

Citation:
Nie, Y., Y. Zhang, G. Chen, X.-Q. Yang, and D. A. Burrows (2014), Quantifying barotropic and baroclinic eddy feedbacks in the persistence of the Southern Annular Mode, *Geophys. Res. Lett.*, *41*, doi:10.1002/2014GL062210.

Received 14 OCT 2014
Accepted 10 NOV 2014
Accepted article online 13 NOV 2014

Quantifying barotropic and baroclinic eddy feedbacks in the persistence of the Southern Annular Mode

Yu Nie[1], Yang Zhang[1], Gang Chen[2], Xiu-Qun Yang[1], and D. Alex Burrows[2]

[1]Institute for Climate and Global Change Research, School of Atmospheric Sciences, Nanjing University, Nanjing, China, [2]Department of Earth and Atmospheric Sciences, Cornell University, Ithaca, New York, USA

Abstract Understanding the persistence of the Southern Annular Mode (SAM) is important for the intraseasonal and decadal predictability of SAM. Using the ERA-40 and ERA-Interim reanalysis data, this study introduces a new method to quantify the relative roles of barotropic and baroclinic eddy feedbacks in the SAM persistence. Through a hybrid Eulerian-Lagrangian Finite Amplitude Wave Activity diagnostic, it is found that (i) transient wave activity is important in driving the SAM, but it provides a negative feedback to the SAM persistence. (ii) Irreversible potential vorticity mixing, through barotropic processes in the upper troposphere, plays an important role in driving and sustaining the SAM variability. Particularly, following the poleward shift of the eddy-driven jet, the reduction/enhancement in effective diffusivity on the jet's poleward/equatorward flank can be understood by a stronger/weaker zonal jet acting as a robust/leaky mixing barrier. (iii) Baroclinic eddy generation and vertical wave propagation mainly act to sustain the SAM variability.

1. Introduction

The Southern Annular Mode (SAM) is the dominant mode of extratropical variability in the Southern Hemisphere on the intraseasonal time scale. It often exhibits an equivalent barotropic dipolar structure in latitude and represents a meridional shift of the eddy-driven jet. The SAM is more persistent than typical synoptic eddies, as a result of a positive feedback between the eddy momentum forcing and anomalous zonal flow [e.g., *Lorenz and Hartmann*, 2001]. Understanding the mechanisms that determine the positive eddy feedback has important implications for the intraseasonal and decadal predictability of SAM [*Gerber et al.*, 2008, 2010].

Barotropic and baroclinic mechanisms have been proposed to understand the positive eddy feedback in the SAM variability. On the one hand, the barotropic mechanism attributes the change of the eddy momentum forcing to the change in barotropic processes, including the anomalous meridional wave propagation and breaking in the upper troposphere, and the resultant irreversible potential vorticity (PV) mixing. In the positive phase of the SAM, the poleward shifted jet leads to more equatorward wave propagation, breaking, and irreversible PV mixing, which further pushes the zonal wind poleward. The response of the anomalous barotropical processes to the SAM variability has been explained from different dynamical aspects, including changes in the refractive index [*Hartmann and Lo*, 1998; *Lorenz and Hartmann*, 2001], the type of wave breaking [*Wang and Magnusdottir*, 2011], and the critical layer behavior [*Chen et al.*, 2008]. On the other hand, the baroclinic mechanism emphasizes the role of the anomalous baroclinic eddy generation in the lower troposphere in the change of the eddy momentum forcing [*Robinson*, 1996]. Following the poleward shift of the zonal jet, the lower tropospheric baroclinic zone and associated baroclinic eddy generation shift poleward. These baroclinic processes, through the upward eddy propagation, couple with the upper level barotropic processes and in turn lead to a poleward shift of the eddy momentum flux [*Robinson*, 2000; *Lorenz and Hartmann*, 2001; *Chen and Plumb*, 2009; *Kidston et al.*, 2010; *Zhang et al.*, 2012]. Particularly, the latitudinal shift of the lower tropospheric baroclinic zone following the jet shift has been explained by the role of surface friction [*Robinson*, 1996; *Chen and Plumb*, 2009], synoptic eddy-induced mean meridional circulation [*Robinson*, 2000; *Gerber and Vallis*, 2007; *Blananco-Fuentes and Zurita-Gotor*, 2011] and the direct heat transport by low-frequency eddies [*Zhang et al.*, 2012; *Nie et al.*, 2013].

Although as suggested in the above mechanism studies, the positive eddy feedback in the SAM can be attributable to the change in barotropic process as the upper level irreversible PV mixing and the change in baroclinic process as the lower level baroclinic eddy generation, it remains unknown on the relative

importance of the barotropic and baroclinic processes in the annular mode variability. Quantifying eddy feedback strength by the irreversible PV mixing and baroclinic eddy generation is the key to answer this question. Recent study by *Nakamura and Zhu* [2010] introduced a finite amplitude wave activity (FAWA hereafter) analysis, which proves to be very efficient in quantifying the eddy-zonal flow interaction in an idealized baroclinic eddy life cycle [*Solomon et al.*, 2012] and in the atmospheric response to climate forcing [*Chen et al.*, 2013; *Sun et al.*, 2013; *Lu et al.*, 2013]. In the formalism, contributions of irreversible PV mixing and baroclinic eddy generation to the eddy momentum forcing can be explicitly diagnosed. This study will apply the FAWA analysis to quantify the relative contributions of barotropic and baroclinic processes in the eddy feedbacks to the SAM persistence.

The structure of this paper is organized as follows. Data and analysis methods used in this study are described in section 2. The relative contributions of barotropic versus baroclinic feedbacks in the SAM persistence are analyzed and discussed in section 3. A brief summary and discussion are provided in section 4.

2. Data and Methodology

2.1. Reanalysis Data

In this study, we use 44 year (1958–2001) European Center for Medium-Range Weather Forecasts (ECMWF) reanalysis (ERA-40) 2.5° × 2.5° latitude-longitude gridded daily (1200 UTC) data at constant pressure levels [*Uppala et al.*, 2005] from 100 hPa to the surface. To analyze the variability of the atmosphere, the full year daily anomaly data for the Southern Hemisphere are used. The daily anomaly is computed by removing the mean seasonal cycle, which is defined as the annual average plus the first four Fourier harmonics of the daily climatology. The SAM in this study is described by the leading empirical orthogonal function (EOF) of the vertically averaged zonal mean daily anomalous zonal wind from 30°S to 70°S. For the EOF analysis, the anomalous zonal wind is properly weighted by the square root of the cosine of latitude [*North et al.*, 1982] to account for the decrease of area toward the pole. All the analysis shown in this work were also checked using the 35 year (1979–2013) 1.5° × 1.5° latitude-longitude gridded ERA-Interim data set produced by ECMWF [*Dee et al.*, 2011] to guarantee the robustness of the results.

2.2. FAWA

Nakamura and Zhu [2010] defined the FAWA by the waviness of quasi-geostrophic potential vorticity (PV, denoted by q) contours at a constant pressure level.

$$A = \frac{1}{2\pi a \cos\phi_e}\left(\iint_{q>Q,\ \phi\le\phi_e(Q)} q\mathrm{d}S - \iint_{q\le Q,\ \phi>\phi_e(Q)} q\mathrm{d}S\right), \tag{1}$$

where ϕ denotes latitude and the area element $\mathrm{d}S = a^2\cos\phi\mathrm{d}\lambda\mathrm{d}\phi$. Here ϕ_e is the equivalent latitude corresponding to the contour $q = Q$, as determined by the requirement that the area enclosed by the PV contour Q toward the polar cap equals the area poleward of ϕ_e. An example of the diagnostic is shown by the PV field at 300 hPa in Figure 1a, where the solid black line denotes the PV contour and the magenta dashed line denotes the corresponding equivalent latitude. For the Q contour in black, the wave activity is calculated by q integrated, from the equivalent latitude, over the equatorward flow in blue minus q integrated over the poleward flow in red. As such, the wave activity describes the net areal displacement of the potential vorticity contour from the zonal symmetry. This is well defined in spite of overturning and cutoffs in PV contours. It is also noteworthy that the instantaneous latitudinal distribution of wave activity A exhibits maxima at the jet flanks and a minimum at the jet center (Figure 1b). This is consistent with the notion that large wave activity is accompanied by the zonal wind deceleration through eddy-zonal flow interactions.

Following the formalism of *Nakamura and Zhu* [2010], *Chen et al.* [2013] showed that the eddy momentum flux convergence can be written as

$$M \equiv -\frac{1}{a\cos^2\phi}\frac{\partial([u^*v^*]\cos^2\phi)}{\partial\phi} = \underbrace{-\frac{\partial}{\partial p}\left(\frac{f[v^*\theta^*]}{\partial\theta_s/\partial p}\right)}_{\text{baroclinic}} \underbrace{-\frac{k_{\text{eff}}}{a}\frac{\partial Q}{\partial\phi_e}}_{\text{barotropic}} - \frac{\partial A}{\partial t} + \Delta\Sigma, \tag{2}$$

where * denotes the eddy component and [ ] denotes the zonal average. The first term on the right-hand side (RHS) of the equation is the vertical convergence of eddy heat flux divided by the static stability parameter (hereafter denoted as baroclinic term), representing the baroclinic processes as the lower level

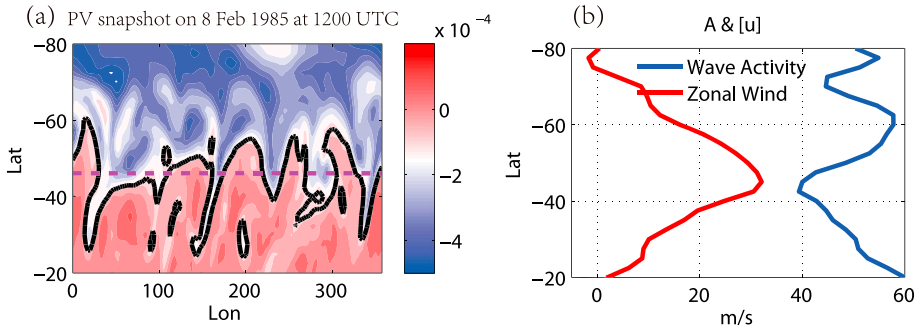

Figure 1. (a) Longitude-latitude snapshot of PV field at 300 hPa on 8 February 1985 1200 UTC (unit: s^{-1}). The black contour denotes the PV value corresponding to the equivalent latitude highlighted by the magenta dashed line. The area enclosed by the black line toward the polar cap equals the area poleward of magenta line. (b) The zonal wind $[u]$ and finite amplitude wave activity A at the same moment.

baroclinic eddy generation and vertical wave propagation [*Edmon et al.*, 1980]. In the steady state of a conservative (i.e., adiabatic and frictionless) flow, the eddy momentum flux convergence is totally determined by the vertical convergence of wave activity flux from lower levels: $M = -\frac{\partial}{\partial p}\left(\frac{f[v^*\theta^*]}{\partial\theta_s/\partial p}\right)$. The second term on the RHS of the equation (hereafter denoted as barotropic term) represents the irreversible PV mixing and is expressed by a diffusive closure. The irreversible PV mixing represents the barotropic processes such as upper tropospheric wave breaking and filamentation that lead to wave activity dissipation at small scales, and k_{eff} denotes the effective diffusivity of irreversible PV mixing [*Nakamura*, 1996]. Large values of k_{eff} are expected in the region of wave breaking (e.g., the jet flanks in Figure 1a), where the filamentation of PV contours enhances the small-scale diffusion. In this study, k_{eff} is estimated as a residual using equation (2). The third term on the RHS of equation (2) is the negative time tendency of wave activity A. In the limit of a pure barotropic conservative flow, $A + [u]$ is constant even if nonlinear wave breaking occurs, as expected from Kelvin's circulation theorem [*Nakamura and Zhu*, 2010]. This term indicates that an increase of wave activity on the jet's equatorward flank or a decrease on the poleward flank will lead to a poleward shift in the jet. Finally, $\Delta\Sigma$ denotes the diabatic source/sink of wave activity. This term is ignored in our study, as the diabatic heating is relatively weak in the upper troposphere. In summary, equation (2) provides a framework to quantify the roles of baroclinic and barotropic processes in the eddy momentum forcing. Note that this is a hybrid Eulerian-Lagrangian diagnostic: the eddy flux is local in latitude, but the wave activity and PV gradient are evaluated following the PV contours.

2.3. Quantifying Eddy Feedbacks by Barotropic and Baroclinic Processes

Consider the vertically averaged zonal momentum budget under the quasi-geostrophic approximation,

$$\frac{\partial\langle[u]\rangle}{\partial t} = < M > -\langle[F_r]\rangle, \tag{3}$$

where $\langle\ \rangle$ denotes the vertical average and F_r denotes the boundary layer friction. This indicates the changes of the extratropical zonal wind are directly driven by the eddy momentum flux convergence and damped by the surface friction. The eddy momentum forcing can be divided into two parts: the part from the upper level eddy momentum flux, which is defined as $< M >_{\mathrm{up}} = \frac{1}{1000\ \mathrm{hPa}-100\ \mathrm{hPa}}\int_{100\ \mathrm{hPa}}^{500\ \mathrm{hPa}} M dp$ and the part from the contribution of lower levels, defined as $< M >_{\mathrm{low}} = \frac{1}{1000\ \mathrm{hPa}-100\ \mathrm{hPa}}\int_{500\ \mathrm{hPa}}^{1000\ \mathrm{hPa}} M dp$. In the observations, the eddy momentum flux is mainly confined in the upper troposphere (i.e., $< M > \approx < M >_{\mathrm{up}}$).

To further quantify the eddy feedbacks in the SAM, we project the zonal momentum equation (3) onto the normalized leading EOF of the barotropic zonal wind.

$$\frac{\partial z}{\partial t} = m - \frac{z}{D} \approx m_{\mathrm{up}} - \frac{z}{D}, \tag{4}$$

where $z(t)$ is the leading principal component time series of the barotropic zonal wind (UPC1) and defined with unit of m s^{-1}. m and m_{up} are the corresponding projection time series of the vertically averaged eddy momentum forcing $< M >$ and upper level eddy momentum forcing $< M >_{\mathrm{up}}$. D is the frictional damping timescale.

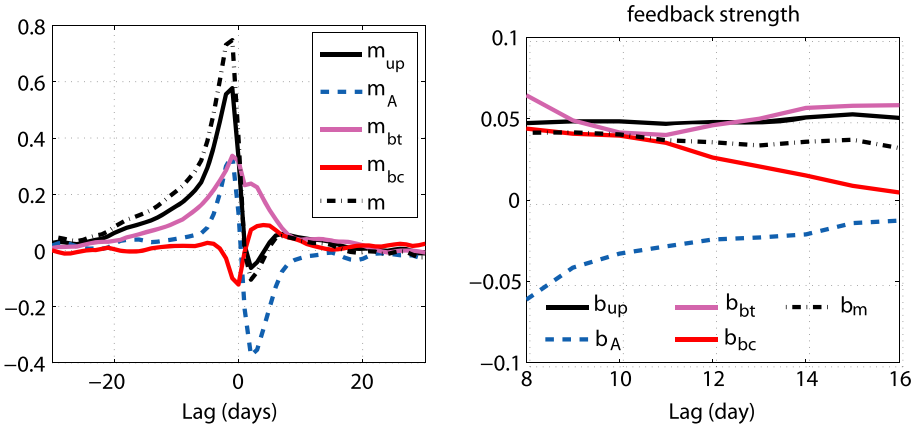

Figure 2. (a) Lagged covariance between the time series of upper tropospheric (500–100 hPa) averaged FAWA budget and the leading PC time series of $\langle [u] \rangle$ (Unit: (m s^{-1})^{2}d^{-1}). Positive lags denote that the zonal wind leads the forcing. (b) Upper tropospheric eddy feedback strengths over lags + 8 to +16 days (Unit: day^{-1}). The dash-dotted line denotes the 1000–100 hPa vertically averaged eddy momentum forcing.

The upper level eddy momentum forcing, m_{up}, can be interpreted by projecting the upper tropospheric average of the FAWA equation (2) onto the same barotropic zonal wind EOF.

$$m_{\mathrm{up}} = m_{\mathrm{bc}} + m_{\mathrm{bt}} + m_A, \tag{5}$$

where m_{bc}, m_{bt}, and m_A are the corresponding projection time series of baroclinic and barotropic terms and wave activity tendency in the FAWA equation.

As in *Lorenz and Hartmann* [2001], $m_{\mathrm{up}}(t)$ can be parameterized as the random momentum forcing $\tilde{m}_{\mathrm{up}}$ plus the zonal flow feedback part $b_{\mathrm{up}}z$, in which b_{up} denotes the eddy momentum feedback strength. Then, the total upper tropospheric eddy momentum forcing time series m_{up} can be decomposed as

$$m_{\mathrm{up}} = \tilde{m}_{\mathrm{up}} + b_{\mathrm{up}}z = \tilde{m}_{\mathrm{up}} + b_{\mathrm{bc}}z + b_{\mathrm{bt}}z + b_A z, \tag{6}$$

where b_{bc}, b_{bt}, and b_A denote the eddy feedbacks due to baroclinic processes, barotropic processes, and wave activity tendency, respectively. The feedback strengths can be estimated through a lagged regression analysis, as described in *Simpson et al.* [2013]. The time series m_{up} and z are regressed onto z with a lag of Δt: $m_{\mathrm{up}}(t + \Delta t) \approx \beta_m^{\Delta t} z(t)$ and $z(t + \Delta t) \approx \beta_z^{\Delta t} z(t)$, where $\beta_m^{\Delta t}$ and $\beta_z^{\Delta t}$ are the regression coefficients of m_{up} and z at the lag Δt. As the eddy momentum forcing is mainly organized by the zonal flow at large lags, the regressed component of the random part of eddy momentum forcing for large Δt should be zero. Hence, the eddy momentum feedback strength can be obtained by $b_{\mathrm{up}}^{\Delta t} = \beta_m^{\Delta t} / \beta_z^{\Delta t}$. Similarly, by replacing m_{up} with m_{bc}, m_{bt}, and m_A, the eddy feedback strength of the baroclinic process b_{bc}, barotropic process b_{bt}, and wave activity tendency b_A can be estimated with this linear feedback model.

3. Results

3.1. Quantifying Barotropic and Baroclinic Eddy Feedbacks

First, the upper tropospheric (500–100 hPa) averaged eddy forcing time series is calculated by projecting each term in equation (2) onto the normalized leading EOF of the barotropic zonal wind. Figure 2a shows the lagged covariance between the eddy forcing time series and $z(t)$. As pointed out by *Lorenz and Hartmann* [2001], when the zonal wind leads eddy momentum forcing around 8–16 days, the persistent positive covariances indicate a positive feedback between the eddy momentum forcing and the zonal wind anomaly. The FAWA analysis facilitates a separation between barotropic and baroclinic processes in the life cycle of SAM. At negative lags, the strong positive covariance between the time series of the barotropic term in equation (2) and $z(t)$ suggests a strong driving effect of barotropic processes in the SAM variability. The negative wave activity tendency also drives the zonal wind variability. This is analogous to the conservation of $[u] + A$ for a barotropic flow, which indicates an out-of-phase relationship between the zonal wind and wave activity. In contrast, the wave activity flux from the lower troposphere plays a negligible role. Furthermore, at relatively large positive lags (around 8–16 days), both the barotropic and baroclinic terms are

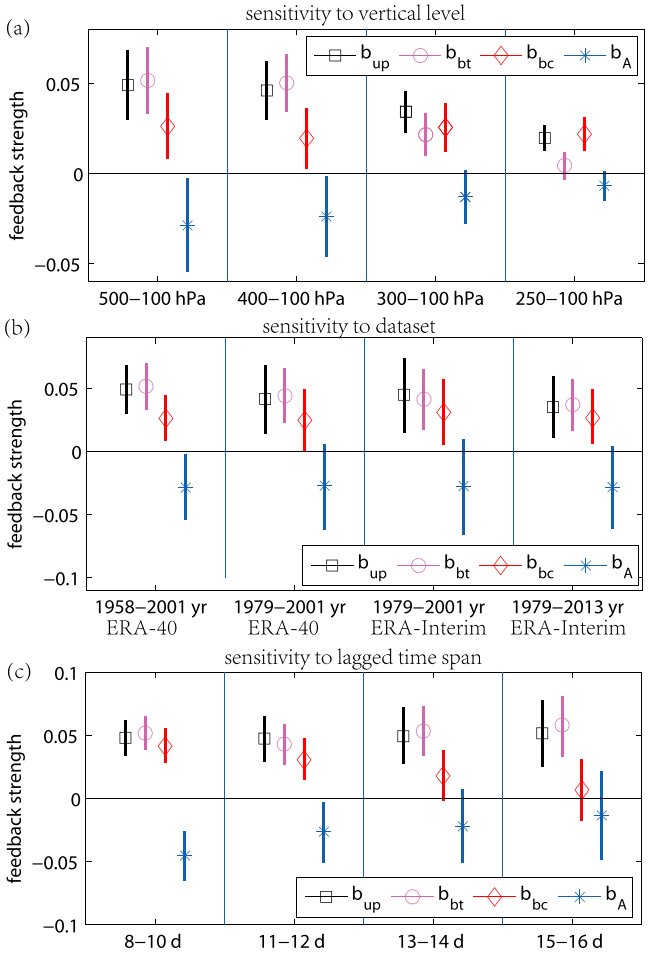

Figure 3. (a) The eddy feedback strength averaged over different vertical levels. (b) The eddy feedback strength at ERA-40 and ERA-Interim data sets over different time spans. (c) The eddy feedback strength at different time lag. (Unit: day^{-1}). The 95% confidence intervals on the estimates of feedback strength are also calculated using the same method as in *Simpson et al.* [2013].

positively correlated with the zonal wind anomaly, indicating that both of them contribute to the positive feedback between the eddy momentum forcing and the anomalous zonal wind. The wave activity tendency, however, is negatively correlated with the anomalous zonal wind, indicating a negative feedback to the SAM variability.

Using the method described in section 2.3, the feedback strength attributable to the barotropic and baroclinic processes is quantified. Figure 2b shows the upper tropospheric (500–100 hPa) averaged eddy feedback strength as a function of lag, Δt, when the zonal wind leads the eddy forcing by 8 to 16 days. As suggested by *Simpson et al.* [2013], the almost constant positive values at long positive lags between the eddy momentum forcing and the zonal wind anomaly represent a positive eddy feedback, indicating that the linear feedback model in equation (6) works well in describing the eddy feedback. The eddy momentum feedback strength averaged over 1000 to 100 hPa is also plotted in Figure 2b for comparison, which shows that the total vertically averaged eddy momentum feedback is mostly from the contributions of upper troposphere.

Figure 2b also compares the eddy feedback strength by barotropic and baroclinic processes as well as the wave activity tendency. The barotropic process almost dominates the total positive eddy feedback. The contribution from the baroclinic process is weaker but still of the same order as that by the barotropic process. The positive feedbacks are offset by the negative feedback induced by the wave activity tendency. In addition, the feedback strength resulting from the vertical wave activity convergence decreases with larger lag, indicating that there might be some limitation using the linear model to describe the baroclinic feedback. This sensitivity of the positive baroclinic feedback to the lag used in the regression analysis is greatly canceled by the negative feedback due to the wave activity tendency. The barotropic feedback is relatively insensitive to the lag.

3.2. Sensitivities of the Feedback Analysis

Figure 3 investigates the sensitivities of the feedback strength to the vertical levels, data set, and time lag, in which the feedback strength is also quantified with 95% confidence limits calculated with the same method as in *Simpson et al.* [2013]. First, the same feedback analysis is carried out as in section 3.1, but each eddy forcing term is averaged over 500–100, 400–100, 300–100, and 250–100 hPa. Figure 3a displays the eddy feedback strength for the individual terms in equation (6) and the feedback strength is averaged over lag +8 to +16 days. While the strength of the feedback due to baroclinic process does not change much with the depth of vertical levels, the barotropic feedback increases with a deeper vertical average and levels off as the lower boundary is below 400 hPa. This suggests that the barotropic eddy feedback is mostly confined from 400 hPa to the tropopause. The negative feedback of wave activity transience also increases with a deeper

vertical average. This is mainly due to its fairly barotropic structure in the upper troposphere, which will be further discussed in the following section.

Next, the feedback analysis is repeated using the ERA-Interim data set and different periods of reanalysis data (Figure 3b). While there is a minor change in eddy feedback strength by a change of the data set or the average period, the results are generally consistent: the feedback strength from barotropic processes is larger than the contribution from baroclinic processes and the wave activity tendency acts as a negative feedback to the SAM variability.

Finally, the sensitivity of the feedback strength to the average period is displayed in Figure 3c. Consistent with Figure 2b, the total and barotropic feedback strengths stay roughly constant for different periods within lag 8 to 16 days. In contrast, the eddy feedback strengths due to baroclinic processes and wave activity tendency vary with the chosen average period, with a weaker feedback at larger time lags. This indicates the wave activity tendency is more related to the vertical convergence of wave activity rather than the meridional divergence, which is consistent with the study by *Pfeffer* [1987].

3.3. Mechanisms of Barotropic and Baroclinic Feedbacks

Figures 4a and 4b show the regression pattern with respect to normalized $z(t)$ for the zonal wind at lag day 0 and anomalous *E-P* flux cross section at lag 10 days. The 10 day lag is used to eliminate the random fluctuations in eddy forcing. Consistent with *Lorenz and Hartmann* [2001], the poleward shift in zonal wind at lag day 0 is reinforced by the anomalous *E-P* flux forcing at lag day 10, with enhanced wave generation and anomalous upward wave propagation on the poleward side of jet, and reduced wave generation as well as anomalous downward propagation on the equatorward side.

The mechanisms of barotropic and baroclinic eddy feedbacks to the anomalous zonal wind are elucidated by regressing each term in the FAWA budget equation (2) onto normalized $z(t)$ with a 10 day lag. The regression pattern of the eddy momentum flux convergence displays a dipolar structure in latitude, acting to enhance the poleward shift of the westerly jet (Figure 4c). This, however, cannot be explained by transient wave activity (Figure 4d), which is opposite in sign to the anomalous momentum flux convergence. In other words, the positive eddy feedback in the SAM variability cannot be explicated by the conservation of $[u] + A$ in barotropic dynamics alone.

The regression pattern of the irreversible PV mixing in the upper troposphere is illustrated in Figure 4e. Similar to the eddy momentum forcing, the dipolar structure of the anomalous PV mixing reinforces the eddy-driven jet in the positive phase of SAM. The regressed pattern of the effective eddy diffusivity is also plotted in Figure 4g, which approximately shows a reduction/enhancement in upper tropospheric effective diffusivity at lag day 10, where the anomalous zonal wind is positive/negative at lag day 0. This can be understood by that the upper tropospheric zonal jet acts as a mixing barrier [e.g., *Nakamura*, 1996; *Haynes and Shuckburgh*, 2000] and that the latitudinal shift in jet also leads to a latitudinal shift in eddy mixing as well as eddy dissipation.

The change in effective diffusivity can be also linked to the change in Rossby wave breaking (RWB) frequency. Following the algorithm of *Rivière* [2009], the RWB event is detected by counting the point where a PV contour has a local reversal. Then the regression pattern of the RWB frequency with respect to normalized $z(t)$ with a 10 day lag is presented in Figure 4h. As expected, the RWB frequency also exhibits a strong reduction on the poleward side of the jet and an enhancement on the equatorward side, similar to *Wang and Magnusdottir* [2011], which is roughly consistent with the change of the effective diffusivity. There are also some disagreements, as expected, between the two diagnostics, since the RWB detection does not distinguish large and small reversal events but the effective diffusivity can be thought of as the length of the PV contours that depends on the extent of the reversal.

The role of the baroclinic processes in the positive eddy feedback is displayed in Figure 4f. In spite of a more complex structure, the regression pattern above 400 hPa can be roughly described by anomalous vertical convergence on the poleward side of jet and vertical divergence on the equatorward side. In conjunction with Figure 4b, this indicates a poleward shift of the baroclinic eddy generation, supporting the more equatorward wave propagation in the upper troposphere.

In summary, the positive eddy feedbacks in the SAM can be understood in the FAWA framework as follows. On the one hand, in the positive phase of SAM, the poleward shifted upper tropospheric jet suppresses the PV mixing on the jet's poleward side, the eddy dissipation on the poleward side is inhibited, and the Rossby

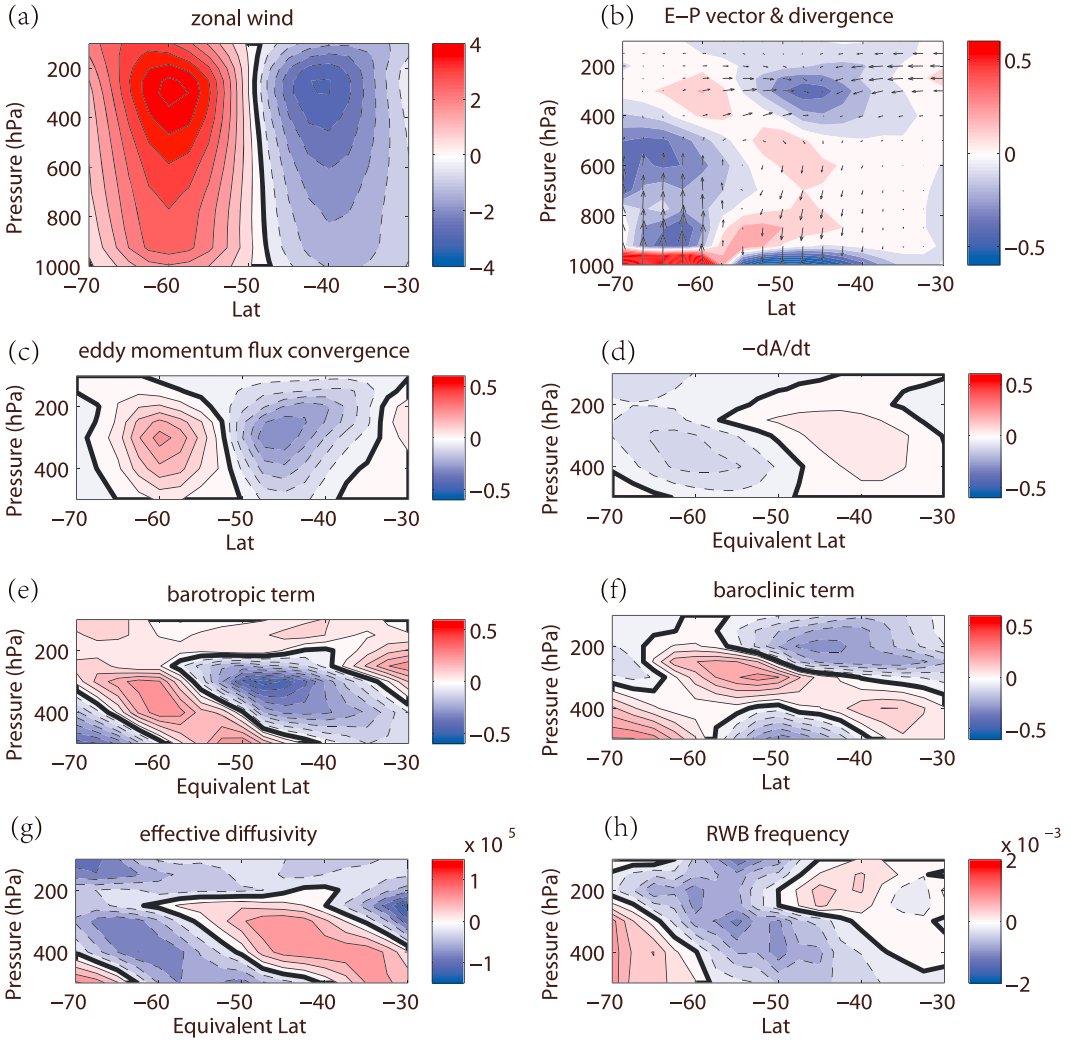

Figure 4. Lagged regression pattern with respect to normalized $z(t)$ for the (a) zonal wind (interval: 0.5 m s^{-1}) at lag day 0 and (b) anomalous *E-P* flux and its divergence (shading, interval: 0.1 m s^{-1} d^{-1}) at lag 10 days. Lagged regressions of the upper tropospheric (500–100 hPa) FAWA budget and Rossby wave breaking frequency onto normalized $z(t)$ when zonal wind leads by 10 days: (c) the eddy momentum flux convergence, (d) negative time tendency of wave activity, (e) barotropic term (dissipation of wave activity), (f) baroclinic term (eddy heat flux vertical convergence), (g) effective diffusivity (interval: 2×10^4 m^2 s^{-1}), and (h) Rossby wave breaking frequency (interval: 0.0002 day^{-1}). The contour interval in Figures 4c–4f is 0.05 $m^1 s^{-1} d^{-1}$.

wave is in favor of propagating and breaking more equatorward. On the other hand, anomalous baroclinic eddy begins to generate on the poleward side of the jet, providing more waves propagating upward and away from the source region. Both the barotropic and baroclinic processes provide positive feedbacks to the anomalous zonal wind.

4. Conclusions and Discussion

Using the ERA-40 and ERA-Interim reanalysis data, this study quantifies the relative roles of barotropic and baroclinic processes in sustaining the positive feedback between eddy momentum forcing and anomalous zonal wind in the SAM variability. Our new analysis shows that both the barotropic and baroclinic processes proposed in the previous mechanism studies are significant for the persistence of the SAM. It is further found that

1. Transient wave activity is important, as expected from the conservation of $[u] + A$ in barotropic dynamics, in driving the SAM, but it provides a negative feedback to the SAM persistence.

2. Irreversible PV mixing, through barotropic processes such as wave breaking and filamentation in the upper troposphere, plays an important role in driving and sustaining the SAM variability. Particularly, following the poleward shift in the eddy-driven jet, the reduction/enhancement in effective diffusivity on the jet's poleward/equatorward flank can be understood by a stronger/weaker zonal jet acting as a robust/leaky mixing barrier [e.g., *Nakamura*, 1996; *Haynes and Shuckburgh*, 2000].
3. Baroclinic eddy generation and vertical wave propagation mainly act to sustain the anomalous zonal wind in SAM. The magnitude of the eddy feedback by baroclinic process is in general weaker than the barotropic one, but still important for the SAM persistence.

The FAWA framework is highlighted in our study in understanding the eddy-mean flow interactions in the low-frequency variability of the zonal flow. Although as suggested in the previous studies, the baroclinic and barotropic processes are often coupled in the SAM variability [*Robinson*, 1996, 2000], the contributions of the two processes can be evidently separated in the FAWA budget. With this hybrid Eulerian-Lagrangian diagnostic approach, both the barotropic and baroclinic dynamics in sustaining the positive eddy feedback in the SAM can be explicitly diagnosed and quantitatively compared through our proposed linear feedback model. We emphasize that the baroclinic eddy feedback quantified in our methodology, instead of directly corresponding to the baroclinic feedback mechanism associated with the mean meridional circulation response to an upper tropospheric wave drag [i.e., *Robinson*, 2000], actually accounts for all the baroclinic changes in the lower levels contributing to the eddy momentum forcing. We noted that previous studies also suggest that eddies with different length and time scales act differently to the SAM persistence, e.g., *Simpson et al.* [2013] identified a negative feedback of the barotropic planetary-scale eddies for the jet variability and *Nie et al.* [2013] showed the different roles of synoptic and low-frequency eddies for the baroclinic anomalies associated with SAM. How to quantify the contributions of different eddies via barotropic and baroclinic processes to the total eddy feedback will be a future topic to develop the FAWA approach to diagnosing the annular mode dynamics.

Diagnosing the barotropic and baroclinic eddy feedbacks in the annular modes is suggested helpful in understanding the overestimated persistence of the annular mode in comprehensive climate models [*Gerber et al.*, 2008; *Zurita-Gotor et al.*, 2013], the variations of the annular mode in the context of climate change [*Barnes and Hartmann*, 2010; *Barnes and Polvani*, 2013], or the response of midlatitude weather to recent Arctic amplification [*Cohen et al.*, 2014]. It is expected that the FAWA diagnostic approach proposed in this study will shed new insights in the questions above.

Acknowledgments
We thank the two anonymous reviewers for their constructive suggestions. The ERA-40 and ERA-Interim reanalysis used in this study were obtained from http://www.ecmwf.int/en/research/climate-reanalysis/browse-reanalysis-datasets. This study was supported by the NSF of China under grants 41275058, 41005028, and 41330420. G.C. and D.A.B. are supported by the U.S. NSF award AGS-1248201.

The Editor thanks two anonymous reviewers for their assistance in evaluating this paper.

References

Barnes, E. A., and D. L. Hartmann (2010), Testing a theory for the effect of latitude on the persistence of eddy driven jets using CMIP3 simulations, *Geophys. Res. Lett.*, *37*, L15801, doi:10.1029/2010GL044144.

Barnes, E. A., and L. Polvani (2013), Response of the midlatitude jets, and of their variability, to increased greenhouse gases in the CMIP5 models, *J. Clim.*, *26*, 7117–7135.

Blananco-Fuentes, J., and P. Zurita-Gotor (2011), The driving of baroclinic anomalies at different time scales, *Geophys. Res. Lett.*, *38*, L23805, doi:10.1029/2011GL049785.

Chen, G., and R. Plumb (2009), Quantifying the eddy feedback and the persistence of the zonal index in an idealized atmospheric model, *J. Atmos. Sci.*, *66*, 3707–3720.

Chen, G., J. Lu, and D. M. Frierson (2008), Phase speed spectra and the latitude of surface westerlies: Interannual variability and global warming trend, *J. Clim.*, *21*, 5942–5959.

Chen, G., J. Lu, and L. Sun (2013), Delineating the eddy-zonal flow interaction in the atmospheric circulation response to climate forcing: Uniform SST warming in an idealized aqua-planet model, *J. Atmos. Sci.*, *70*, 2214–2233.

Cohen, J., et al. (2014), Recent Arctic amplification and extreme mid-latitude weather, *Nat. Geosci.*, *7*, 627–637, doi:10.1038/ngeo2234.

Dee, D., S. Uppala, A. Simmons, P. Berrisford, P. Poli, S. Kobayashi, U. Andrae, M. Balmaseda, G. Balsamo, and P. Bauer (2011), The ERA-interim reanalysis: Configuration and performance of the data assimilation system, *Q. J. R. Meteorol. Soc.*, *137*, 553–597.

Edmon, H., B. Hoskins, and M. McIntyre (1980), Eliassen-Palm cross sections for the troposphere, *J. Atmos. Sci.*, *37*, 2600–2616.

Gerber, E., and G. Vallis (2007), Eddy-zonal flow interactions and the persistence of the zonal index, *J. Atmos. Sci.*, *64*, 3296–3311.

Gerber, E., L. Polvani, and D. Ancukiewicz (2008), Annular mode time scales in the intergovernmental panel on climate change fourth assessment report models, *Geophys. Res. Lett.*, *35*, L22707, doi:10.1002/grl.50649.

Gerber, E. P., M. P. Baldwin, H. Akiyoshi, J. Austin, S. Bekki, P. Braesicke, N. Butchart, M. Chipperfield, M. Dameris, and S. Dhomse (2010), Stratosphere-troposphere coupling and annular mode variability in chemistry-climate models, *J. Geophys. Res.*, *115*, D00M06, doi:10.1029/2009JD013770.

Hartmann, D., and F. Lo (1998), Wave-driven zonal flow vacillation in the Southern Hemisphere, *J. Atmos. Sci.*, *55*, 1303–1315.

Haynes, P., and E. Shuckburgh (2000), Effective diffusivity as a diagnostic of atmospheric transport: 2. Troposphere and lower stratosphere, *J. Geophys. Res.*, *105*, 22,795–22,810, doi:10.1029/2000JD900092.

Kidston, J., D. Frierson, J. Renwick, and G. Vallis (2010), Observations, simulations, and dynamics of jet stream variability and annular modes, *J. Clim.*, *23*, 6186–6199.

Lorenz, D. J., and D. L. Hartmann (2001), Eddy-zonal flow feedback in the Southern Hemisphere, *J. Atmos. Sci.*, *58*, 3312–3327.

Lu, J., L. Sun, Y. Wu, and G. Chen (2013), The role of subtropical irreversible PV mixing in the zonal mean circulation response to global warming-like thermal forcing, *J. Clim.*, *27*, 2297–2316.
Nakamura, N. (1996), Two-dimensional mixing, edge formation, and permeability diagnosed in an area coordinate, *J. Atmos. Sci.*, *53*, 1524–1537.
Nakamura, N., and D. Zhu (2010), Finite-amplitude wave activity and diffusive flux of potential vorticity in eddy-mean flow interaction, *J. Atmos. Sci.*, *67*, 2701–2716.
Nie, Y., Y. Zhang, X.-Q. Yang, and G. Chen (2013), Baroclinic anomalies associated with the southern hemisphere annular mode: Roles of synoptic and low-frequency eddies, *Geophys. Res. Lett.*, *40*, 2361–2366, doi:10.1002/grl.50396.
North, G., F. Moeng, T. Bell, and R. Cahalan (1982), The latitude dependence of the variance of zonally averaged quantities, *Mon. Weather Rev.*, *110*, 319–326.
Pfeffer, R. L. (1987), Comparison of conventional and transformed Eulerian diagnostics in the troposphere, *Q. J. R. Meteorol. Soc.*, *113*, 237–254.
Rivière, G. (2009), Effect of latitudinal variations in low-level baroclinicity on eddy life cycles and upper-tropospheric wave-breaking processes, *J. Atmos. Sci.*, *66*, 1569–1592.
Robinson, W. A. (1996), Does eddy feedback sustain variability in the zonal index?, *J. Atmos. Sci.*, *53*, 3556–3569.
Robinson, W. A. (2000), A baroclinic mechanism for the eddy feedback on the zonal index, *J. Atmos. Sci.*, *57*, 415–422.
Simpson, I. R., T. G. Shepherd, P. Hitchcock, and J. F. Scinocca (2013), Southern Annular Mode dynamics in observations and models. Part II: Eddy feedbacks, *J. Clim.*, *26*, 5220–5241.
Solomon, A., G. Chen, and J. Lu (2012), Finite-amplitude Lagrangian-mean wave activity diagnostics applied to the baroclinic eddy life cycle, *J. Atmos. Sci.*, *69*, 3013–3027.
Sun, L., G. Chen, and J. Lu (2013), Sensitivities and mechanisms of the zonal mean atmospheric circulation response to tropical warming, *J. Atmos. Sci.*, *70*, 1569–1586.
Uppala, S. M., et al. (2005), The ERA-40 re-analysis, *Q. J. R. Meteorol. Soc.*, *131*, 2961–3012.
Wang, Y.-H., and G. Magnusdottir (2011), Tropospheric Rossby wave breaking and the SAM, *J. Clim.*, *24*, 2134–2146.
Zhang, Y., X.-Q. Yang, Y. Nie, and G. Chen (2012), Annular mode-like variation in a multilayer quasigeostrophic model, *J. Atmos. Sci.*, *69*, 2940–2958.
Zurita-Gotor, P., J. Blanco-Fuentes, and E. P. Gerber (2013), The impact of baroclinic eddy feedback on the persistence of jet variability in the two-layer model, *J. Atmos. Sci.*, *71*, 410–429.